

HOW MAXIMUM ALLOWABLE TENSION OF CABLES AND UMBILICALS IS INFLUENCED BY FRICTION

Magnus Komperød*
 Technological Analyses Centre
 Nexans Norway AS
 P. O. Box 42, 1751 HALDEN
 Norway

ABSTRACT

Direct electrical heating (DEH) is a technology for preventing hydrate formation and wax deposit inside oil and gas pipelines. Nexans Norway AS is researching and developing DEH solutions for deep waters. The company has produced a deep-water DEH piggyback cable that can carry its own weight at 1 070 m water depth. When this DEH system is installed outside the coast of Africa, it will be the world's deepest DEH system.

For deep-water cables, including umbilicals, the maximum allowable tension (MAT) is an important parameter that limits the water depth which the cable can be installed at. As MAT by definition is calculated for straight (non-bent) cables, it can be argued from a theoretical point of view that friction should be disregarded. However, from a practical point of view, one can argue that the cable is rarely perfectly straight, which justifies inclusion of friction.

This paper derives the relation between the cable's axial tension, the axial tensions of the individual cable elements, and friction, with emphasize on how friction influences MAT. Four different approaches for calculating friction's influence on MAT are presented. These approaches range from fully neglecting friction to including the maximum possible friction. Two approaches include friction up to a certain curvature limit, which corresponds to an "almost straight" cable, and neglect the friction for higher curvatures. The most conservative approach gives 19% lower MAT than the least conservative approach for the deep-water DEH piggyback cable.

Keywords: Axisymmetric Analysis; Cable Capacity; Capacity Curve; Cross Section Analysis; Maximum Allowable Tension; Maximum Handling Tension; Offshore Technology; Riser; Subsea Cable; Umbilical.

NOTATION

A_i	Cross section area of each cable element in layer i [m ²].	f_i	Maximum possible friction on each element in cable layer i per unit length of the cable [N/m].
C_i	Total radial contact force per unit length of the cable between cable layers $i - 1$ and i [N/m].	L_i	Pitch length of cable layer i [m].
c_i	Radial contact force per unit length of the cable induced by cable layer i [N/m].	l_i	Length of cable elements in layer i over one pitch length [m].
E_i	E-modulus of cable elements in layer i [Pa].	MAT	Maximum allowable tension of the cable [N].
EA_c	The cable's axial stiffness [N].	N	Number of layers of conductor strands [-].
		n_i	Number of strands in layer i [-].
		R_i	Pitch radius of cable elements in layer i [m].
		r_i	Element radius of cable elements in layer i [m].

*Corresponding author: Phone: +47 69 17 35 39 E-mail: magnus.komperod@nexans.com

SMYS	Specified minimum yield stress [Pa].
T_c	The cable's axial tension [N].
$T_{a,i}$	Axial tension of each cable element in layer i due to axial cable tension [N].
α_i	Pitch angle of cable elements in layer i [rad].
ε_c	Axial cable strain [-].
ε_i	Axial strain of cable elements in layer i [-].
κ_c	The cable's bending curvature [m^{-1}].
κ_c^{limit}	The upper limit of cable bending curvature for which friction is included in calculations of MAT [m^{-1}].
$\kappa_{c,i}$	The cable's bending curvature where cable elements in layer i slip at angle θ [m^{-1}].
$\kappa_{c,i}^{\text{max}}$	The maximum cable bending curvature for which $\sigma_{f,i}$ is to be calculated for cable elements in layer i [m^{-1}].
θ	Angular position of cable element, relative to the center of the cable cross section [rad].
$\sigma_{a,i}$	Contribution to axial stress in cable elements of layer i due to axial tension of the cable [Pa].
$\sigma_{b,i}$	Bending stress in cable elements of layer i due to bending the cable [Pa].
$\sigma_{f,i}$	Contribution to axial stress in cable elements of layer i due to friction when bending the cable [Pa].
$\sigma_{f,i}^{\text{max}}$	Maximum possible contribution to axial stress in cable elements of layer i due to friction when bending the cable [Pa].
$\mu_{i,j}$	Coefficient of friction between elements of layer i and layer j .

Negative values of L_i and α_i indicate left lay direction, and positive values indicate right lay direction.

INTRODUCTION

The world's increasing energy demand, combined with the exhaustion of many easily accessible oil and gas reserves, drives the petroleum industry into deeper waters. Manufacturers of subsea cables and umbilicals are among those who face the technological challenges of increased water depths.

Another significant challenge of offshore petroleum production is that the pipeline content is cooled by

the surrounding water. As the pipeline content drops to a certain temperature, hydrates may be formed and wax may start to deposit inside the pipeline wall. Hydrates and wax may partially, or even fully, block the pipeline. Hydrate formation may start at temperature as high as 25°C, while wax deposit may start at 35-40°C [1].

There are several ways to prevent hydrate formation and wax deposition. An intuitive solution is to apply thermal insulation at the outer surface of the pipeline. However, at long pipelines, low flow rates, or production shut downs, this solution may be insufficient.

When thermal insulation is insufficient, a commonly used approach is to add chemicals to the pipeline in order to reduce the critical temperature for hydrate formation and wax deposition. Methanol or glycol is commonly used [1, 2]. However, as explained in reference [1], adding chemicals has practical as well as environmental disadvantages.

A technology that has emerged over the last years is direct electrical heating (DEH). The first DEH system was installed at Statoil's Åsgard oil and gas field in the Norwegian Sea in year 2000 [3]. Nexans Norway AS qualified the DEH technology together with Statoil and SINTEF.

In DEH systems, the electrical resistance of the steel in the pipeline wall is used as a heating element. A single phase cable, referred to as piggyback cable (PBC), is strapped to the pipeline. In the far end (the end of the pipeline far away from the topside) the PBC is connected ("short circuited") to the pipeline. In the near end (the end of the pipeline close to the topside), a two-phase DEH riser cable is connected to the PBC and the pipeline; one phase of the riser cable is connected to the PBC, and the other phase of the riser cable is connected to the pipeline. When the riser cable is energized topside, energy is transferred through the PBC into the steel of the pipeline wall.

Nexans Norway AS is currently developing deep-water DEH solutions. A piggyback cable that is repairable, i.e. can carry its own weight, at 1 070 m water depth is already produced by Nexans in a delivery project. The cross section of this cable is shown in Figure 1. When this DEH system is installed outside the coast of Africa, it will be the world's deepest DEH system [3].

The piggyback cable presented in Figure 1 has 19 (1 + 6 + 12) steel strands in center (gray color in

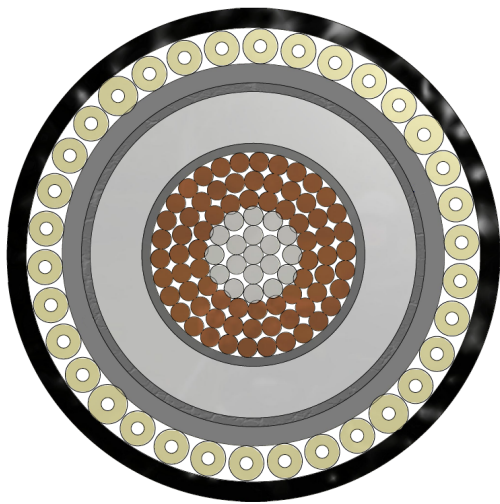


Figure 1: Cross section of the deep-water DEH piggyback cable.

the figure). The purpose of the steel strands is to improve the mechanical capacity of the conductor. This solution is patented by Nexans Norway AS.

Outside the steel strands there are 72 (18 + 24 + 30) copper strands (brown color). Outside the stranded conductor there are an electric insulation system (dark gray and light gray colors) and an inner sheath (gray color). Outside the inner sheath there are fillers for mechanical protection (yellow color), and then the outer sheath (black color).

This paper focuses on how friction influences cables' maximum allowable tension (MAT). This issue is particularly important for deep-water cables and umbilicals. The contributions of the paper are: (i) Derive the relationship between axial cable tension, axial element tension, and friction. This derivation is strongly inspired by references [4], [5], and [6]. (ii) Present four different approaches for how to handle friction when calculating MAT. These four approaches are then compared by applying them to the deep-water DEH piggyback cable and the results are discussed.

The derivations of this paper are based on the following assumptions and simplifications: (i) All materials are assumed to be linear elastic. (ii) Radial displacement and the Poisson ratio effect are neglected. (iii) Helical elements are modeled as tendons. That is, these elements' axial stiffness is modeled, while their bending stiffness and torsion stiffness are neglected. (iv) The cable is prevented from twisting. (v) Only inter-layer contact and friction are

considered, i.e. contact and friction between adjacent cable layers. Intra-layer contact and friction are neglected, i.e. contact and friction within the same cable layer. (vi) When considering radial contact forces, only the steel and copper strands of the piggyback cable is considered, because the radial contact forces caused by the fillers is small compared to those from the strands. (vii) End effects induced in the cable terminations are neglected.

WHY FRICTION INFLUENCES THE MAXIMUM ALLOWABLE TENSION

The technological challenges facing manufacturers of deep-water cables, including umbilicals, are to a large degree caused by the large mechanical forces acting on the cables. The net force of gravity minus buoyancy causes large axial cable tension at hang-off and in the upper part of the cable. The axial cable tension is distributed between the cable elements according to the elements' mechanical properties and the cable geometry.

As many cable elements are helical, large axial cable tension sets up large radial compression forces, which give high friction between the cable elements. When the cable is being bent, the helical elements slide. However, at large axial cable tension, the helical elements stick due to the friction. Then large axial tension and compression forces build up in the elements until the friction is exceeded, and thereby allows the elements to slide. Hence, the axial cable tension gives two contributions to the axial tensions of the cable elements: (i) Distribution of the cable's axial tension to the individual cable elements. (ii) Axial element tensions necessary to exceed the friction.

Large axial cable tension leads to two significant challenges: (i) High axial element tensions may cause the elements to exceed their respective mechanical capacities. (ii) Hanging from topside, the cable is subject to oscillating bending due to waves. Due to high friction, the helical elements partly stick, causing alternating tension and compression. This may lead to fatigue damage of the cable elements. For non-load-carrying elements, both these issues may damage the elements to the extent that they can no longer serve their respective purposes. Even worse is damage to load-carrying elements; this may ultimately break the cable.

This paper focuses on how friction influences the

maximum allowable tension (MAT). MAT is here defined as the maximum axial cable tension, assuming straight (non-bent) cable, where all cable elements are within their respective mechanical capacity criteria. These criteria are typically defined by maximum allowed von Mises stress. If the cable is bent, the cable may be damaged at lower axial tension than MAT.

ELEMENT TENSION VS. CABLE TENSION

In the deep-water DEH piggyback cable of Figure 1, all cable elements are helical, except for the center strand and the sheaths (including the insulation system). All helices have the same center, which is the center of the cable's cross section. While helices are three dimensional geometries, it is common to illustrate these geometries in two dimensions as shown in Figure 2.

The pitch length, L_i , is the axial length of the cable corresponding to one revolution of the helix. Elements in the same cable layer always have the same pitch length. The element length, l_i , is the length of the cable element over one pitch length. The pitch radius, R_i , is the radius from center of the cable to center of the element. The pitch angle, α_i , is the angle between the cable's axis (length direction) and the tangent of the helix. The relation between l_i , L_i , R_i , and α_i is shown in Figure 2.

This section derives the relation between the cable's axial tension, T_c , and the axial tensions of the individual cable elements, $T_{a,i}$. From Figure 2 Pythagoras' theorem gives

$$l_i^2 = (2\pi R_i)^2 + L_i^2. \quad (1)$$

Implicit derivation with respect to L_i

$$2l_i \frac{dl_i}{dL_i} = 2L_i, \quad (2)$$

$$dl_i = \frac{L_i}{l_i} dL_i = \cos(\alpha_i) dL_i. \quad (3)$$

Dividing Eq. 3 by L_i and using $L_i = l_i \cos(\alpha_i)$ gives

$$\frac{dl_i}{L_i} = \frac{dL_i}{l_i \cos(\alpha_i)} = \cos(\alpha_i) \frac{dL_i}{L_i}, \quad (4)$$

$$\frac{dl_i}{l_i} = \cos^2(\alpha_i) \frac{dL_i}{L_i}, \quad (5)$$

$$\varepsilon_i = \cos^2(\alpha_i) \varepsilon_c. \quad (6)$$

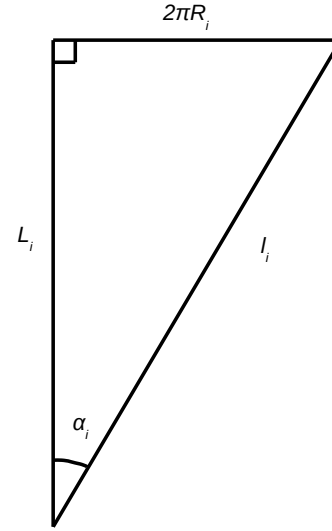


Figure 2: The geometric relation between l_i , L_i , R_i , and α_i .

In Eq. 6 it is used that the cable's axial strain is $\varepsilon_c \stackrel{\text{def}}{=} dL_i/L_i$, while the element's axial strain is $\varepsilon_i \stackrel{\text{def}}{=} dl_i/l_i$. A cable element's axial tension is given as $T_{a,i} = E_i A_i \varepsilon_i$. Hence, multiplying Eq. 6 with $E_i A_i \cos(\alpha_i)$ leads to

$$T_{a,i} \cos(\alpha_i) = E_i A_i \cos^3(\alpha_i) \varepsilon_c, \quad (7)$$

$$\sum_i T_{a,i} \cos(\alpha_i) = \sum_i E_i A_i \cos^3(\alpha_i) \varepsilon_c \quad (8)$$

$$= \left(\sum_i E_i A_i \cos^3(\alpha_i) \right) \varepsilon_c,$$

$$\frac{\sum_i T_{a,i} \cos(\alpha_i)}{\varepsilon_c} = \frac{T_c}{\varepsilon_c} = \sum_i E_i A_i \cos^3(\alpha_i), \quad (9)$$

$$EA_c \stackrel{\text{def}}{=} \frac{T_c}{\varepsilon_c} = \sum_i E_i A_i \cos^3(\alpha_i). \quad (10)$$

In Eq. 8 all cable elements are summed. The strain in the cable's length direction, ε_c , is equal for all cable elements. In Eq. 9 it is used that the cable's axial tension, T_c , is equal to the axial component, $T_{a,i} \cos(\alpha_i)$, of all cable elements. In Eq. 10 it is used the cable's axial stiffness is by definition $EA_c \stackrel{\text{def}}{=} T_c/\varepsilon_c$. Note that Eq. 10 is valid also for non-helical elements. For non-helical elements $\alpha_i = 0$.

Multiplying Eq. 6 with $E_i A_i$ and using $\varepsilon_c = T_c/EA_c$ gives the relation between the cable tension, T_c , and the cable tension's contribution to the elements' ten-

sion, $T_{a,i}$, and axial stress, $\sigma_{a,i}$.

$$E_i A_i \varepsilon_i = E_i A_i \cos^2(\alpha_i) \varepsilon_c, \quad (11)$$

$$T_{a,i} = \frac{E_i A_i \cos^2(\alpha_i)}{E A_c} T_c, \quad (12)$$

$$\sigma_{a,i} = \frac{T_{a,i}}{A_i} = \frac{E_i \cos^2(\alpha_i)}{E A_c} T_c. \quad (13)$$

RADIAL CONTACT FORCES

Figure 3 illustrates a tendon being pulled over the circumference of a circle or a circle sector, for example a rope being pulled over a pulley. If the axial tension of the tendon is T [N] and the radius from center of the circle to the center of the tendon is d [m], then the radial contact force, c [N/m], can be shown to be

$$c = \frac{T}{d} = T \kappa, \quad (14)$$

where $\kappa = \frac{1}{d}$ is the bending curvature of the tendon.

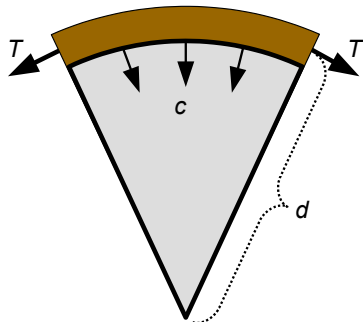


Figure 3: A tendon (brown color) pulled over the circumference of a circle sector (gray color).

For a helix with pitch radius, R , and pitch angle, α , the helix curvature, κ , can be shown to be

$$\kappa = \frac{\sin^2(\alpha)}{R}. \quad (15)$$

Hence, when applying axial tension, T , to a helix wound around a cylindrical core, for example a helical cable element on the beneath cable layer, the radial contact force, c , is

$$c = T \kappa = T \frac{\sin^2(\alpha)}{R}. \quad (16)$$

Eq. 16 expresses the contact force from one cable element per unit length of the element, i.e. along edge

l_i of Figure 2. The contact force per unit length of the cable, i.e. along edge L_i , induced by n_i cable elements is then

$$c_i = \frac{n_i \sin^2(\alpha_i)}{R_i \cos(\alpha_i)} T_{a,i}, \quad (17)$$

$$c_i = \frac{n_i E_i A_i \cos(\alpha_i) \sin^2(\alpha_i)}{R_i E A_c} T_c. \quad (18)$$

Eq. 12 has been inserted into Eq. 17 to give Eq. 18. The contact forces induced by the individual cable layers accumulate, layer by layer, towards the centre of the cable. That is, the contact force between layer N (the outermost layer) and layer $N-1$ is the contact force induced by layer N , i.e. c_N given by Eq. 18. The contact force between layer $N-1$ and layer $N-2$ is the contact force induced by layer $N-1$ and by layer N , i.e. $c_{N-1} + c_N$. Hence, the accumulated contact force acting between layer i and layer $i-1$, C_i , is then

$$C_i = \frac{1}{E A_c} \left(\sum_{j=i}^N \frac{n_j E_j A_j \cos(\alpha_j) \sin^2(\alpha_j)}{R_j} \right) T_c. \quad (19)$$

FRICTION

Assuming Coulomb's friction model, the maximum possible friction force, f [N/m], between two surfaces is $f = \mu c$, where c [N/m] is the normal force and μ [-] is the coefficient of friction.

Except for strands in the the outermost layer and the center strand, all strands are subject to contact forces both from the layer beneath and the layer above. The maximum possible friction force on an element in layer i per length of the element (i.e. along the edge l_i of Figure 2) is then

$$f_i = \frac{\cos(\alpha_i)}{n_i} (\mu_{i,i-1} C_i + \mu_{i,i+1} C_{i+1}). \quad (20)$$

In Eq. 20, the term $\cos(\alpha_i)$ is to give the friction per unit length of the element instead of per unit length of the cable. Division by n_i is to give friction per element.

A common assumption in the literature is to assume that friction has no influence on cables subject to only axisymmetric loads, i.e. axial tension and torsion moment only, see for example reference [6]. However, when the cable is being bent, friction may be very significant, depending on the applied axial tension, the cable geometry, and the material properties. When the cable is bent, the cable itself and

the cable elements are tensioned in the outer arc and compressed in the inner arc.

Reference [7] shows that if a helical cable element is prevented from sliding when the cable is bent, the element's elongation in the outer arc is slightly larger than the contraction in the inner arc. If the helical elements can slide freely, the contraction will completely vanish, and only a tiny elongation will remain. This desired effect is actually one of the main reasons why cables are produced with many cable elements being helical.

If friction is present during cable bending, the helical elements will initially stick. Then axial tension and compression forces build up in the helical elements until the friction is exceeded. When the friction is exceeded, the helical elements slip and move. This behavior is explained in references [4] and [6].

The maximum contributions of friction to the axial stresses in cable elements can be approximated by

$$\sigma_{f,i}^{\max}(\theta) = \frac{R_i \theta}{A_i |\sin(\alpha_i)|} f_i, \quad (21)$$

$$\theta \in \left[-\frac{\pi}{2}, \frac{\pi}{2} \right].$$

In Eq. 21, θ is the helical element's angular position in the cable. For $\theta = 0$ rad the element is at the neutral axis at bending, while for $\theta = \frac{\pi}{2}$ rad the element is at the outer arc at bending, and for $\theta = -\frac{\pi}{2}$ rad the element is at the inner arc. Eq. 21 is derived in references [4] and [6]. The same references also derive an approximation for which cable bending curvature, $\kappa_{c,i}$, the friction is exceeded, i.e. when the helical element starts to slip

$$\kappa_{c,i}(\theta) = \frac{\theta}{E_i A_i \cos^2(\alpha_i) |\sin(\alpha_i)| \sin(\theta)} f_i, \quad (22)$$

$$\theta \in \left[-\frac{\pi}{2}, \frac{\pi}{2} \right].$$

From Eq. 22 it is seen that the first slip occurs at the neutral axis, $\theta = 0$ rad, and then propagates towards the inner arc, $\theta = -\frac{\pi}{2}$ rad, and the outer arc, $\theta = \frac{\pi}{2}$ rad. Also note that the slip propagation reaches the inner arc and the outer arc at a curvature, $\kappa_{c,i}$, that is $\frac{\pi}{2}$ times as large as the curvature of the first slip. Due to symmetry at the point $\theta = -\frac{\pi}{2}$ rad and at the point $\theta = \frac{\pi}{2}$ rad, the behavior explained here will be repeated for every half pitch length of the helical cable element.

FRICITION'S INFLUENCE ON MAXIMUM ALLOWABLE TENSION

Maximum allowable tension (MAT) is an important parameter for deep-water cables, including umbilicals, because MAT limits the water depths which the cables can be installed and operated. MAT is the maximum axial cable tension, T_c , where all cable elements are within their respective criteria for mechanical capacity. These criteria are typically that the element's von Mises stress should be within a certain percentage of the material's specified minimum yield stress (SMYS). MAT is calculated for straight (non-bent) cables. For bent cables the upper limit of axial tension is usually lower than MAT. It is common practice to use a more conservative MAT value during operation than during cable installation.

The following text presents four approaches, with different degree of conservatism, for how to handle friction when calculating or simulating MAT.

Approach 1

As explained above, it is a common assumption in the literature to assume no influence from friction in the axisymmetric case, i.e. when the cable is not bent. Because MAT by definition is calculated for straight cables, it can be argued from a theoretical point of view that friction should be completely neglected when calculating MAT. That is, evaluation of the elements' mechanical capacities are based only on Eq. 12 or Eq. 13, without considering the contribution from Eq. 21. This is the least conservative approach.

Approach 2

From a practical point of view, one can argue that real-life cables are usually not perfectly straight, i.e. have bending curvatures not exactly equal to zero. Based on this point of view, it may be reasonable to include a contribution from friction. A conservative approach will then be to include the maximum possible friction, as given by Eq. 21.

Using this approach, the total axial stress to be evaluated is $\sigma_{a,i} + \sigma_{f,i}^{\max}(\frac{\pi}{2})$, where $\sigma_{a,i}$ is given by Eq. 13 and $\sigma_{f,i}^{\max}$ is given by Eq. 21.

Approach 3

The disadvantage of Approach 1 is that it assumes a perfectly straight cable (exactly zero bending curvature), which may be unrealistic for a real-life cable. Approach 2 includes the maximum possible contribution from friction, regardless of at which cable bending curvature the maximum possible friction is reached. As MAT is defined for non-bent cables, it may be too conservative to include stress from friction occurring at large bending curvatures.

A feasible compromise between Approach 1 and Approach 2 is to include friction up to a certain bending curvature, κ_c^{limit} , which corresponds to an "almost straight" cable, for example $\kappa_c^{\text{limit}} = 1.0 \times 10^{-2} \text{ m}^{-1}$ (i.e. $1.0 \times 10^2 \text{ m}$ bending radius), and neglect friction occurring beyond this curvature.

A cable element is in full slip when Eq. 22 is evaluated for $\theta = \frac{\pi}{2}$ rad. The maximum curvature, $\kappa_{c,i}^{\text{max}}$, for evaluation of $\sigma_{f,i}$ is then the smallest value of Eq. 22 and κ_c^{limit} , i.e.

$$\begin{aligned} \kappa_{c,i}^{\text{max}} & \quad (23) \\ & = \min \left(\frac{\pi}{2E_i A_i \cos^2(\alpha_i) |\sin(\alpha_i)|} f_i, \kappa_c^{\text{limit}} \right). \end{aligned}$$

From reference [6] it follows that until the friction is exceeded, the axial element stress from friction at bending can be approximated by

$$\begin{aligned} \sigma_{f,i}(\theta) & = E_i R_i \cos^2(\alpha_i) \sin(\theta) \kappa_c, \quad (24) \\ \theta & \in \left[-\frac{\pi}{2}, \frac{\pi}{2} \right]. \end{aligned}$$

Eq. 24 is maximized for $\theta = \frac{\pi}{2}$ rad. Then inserting Eq. 23 into Eq. 24 gives the maximum stress due to friction at bending

$$\begin{aligned} \sigma_{f,i} & = E_i R_i \cos^2(\alpha_i) \quad (25) \\ & \times \min \left(\frac{\pi}{2E_i A_i \cos^2(\alpha_i) |\sin(\alpha_i)|} f_i, \kappa_c^{\text{limit}} \right). \end{aligned}$$

If κ_c^{limit} is set to a high value, then $\kappa_{c,i}^{\text{max}}$ is limited by the first term inside the parenthesis of Eq. 23. In this case, Approach 2 and Approach 3 will give the same MAT value. How to decide the value of κ_c^{limit} requires a judgment by the analyst.

The total axial stress to be evaluated is then $\sigma_{a,i} + \sigma_{f,i}$, given by Eq. 13 and Eq. 25, respectively.

Approach 4

The last approach to be discussed in this paper requires a slight re-definition of MAT: Earlier in this paper, MAT was defined as "the maximum axial cable tension, assuming straight (non-bent) cable, where all cable elements are within their respective mechanical capacity criteria". The assumption of straight cable will now be changed to "assuming a small cable bending curvature of κ_c^{limit} ".

This approach has the advantage that MAT can be read directly from the capacity curve. The capacity curve illustrates the allowed combinations of axial cable tension, T_c , and bending curvature, κ_c . Hence, once the capacity curve is established, MAT can be found as the value of T_c corresponding to $\kappa_c = \kappa_c^{\text{limit}}$.

Both Approach 3 and Approach 4 use the curvature limit, κ_c^{limit} . The difference between these two approaches is that Approach 4 also takes into account an additional effect: When the cable is bent, the cable elements are also bent. This introduces bending stresses, $\sigma_{b,i}$, in the cable elements, which are also taken into consideration when evaluating the mechanical strength criteria. Hence, Approach 4 is more conservative than Approach 3.

An expression for bending stress is given in reference [6]. For the deep-water DEH piggyback cable presented in Figure 1, $\sigma_{b,i}$ corresponds to 1-2% of SMYS for the curvature $\kappa_c^{\text{limit}} = 1.0 \times 10^{-2} \text{ m}^{-1}$. Hence, in this case the difference between Approach 3 and Approach 4 is very small.

Comparison of the Four Approaches

Figure 4 compares MAT values of the deep-water DEH piggyback cable presented in Figure 1, using the four approaches explained above. Figure 4 is scaled so that MAT calculated by Approach 1, i.e. the least conservative approach, corresponds to 100%. For Approach 3 and Approach 4 the curvature limit is set to $\kappa_c^{\text{limit}} = 1.0 \times 10^{-2} \text{ m}^{-1}$.

As shown in Figure 4, the most conservative approach (Approach 2) gives 19% lower MAT than the least conservative approach (Approach 1). As expected, there is very good agreement between Approach 3 and Approach 4: Approach 4 is 2% lower than Approach 3.

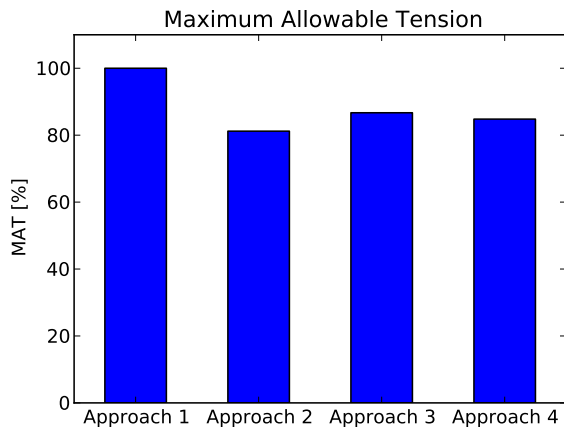


Figure 4: Comparison of approaches 1 through 4 applied to the deep-water DEH piggyback cable presented in Figure 1. The graph is scaled so that MAT calculated by the least conservative approach, i.e. Approach 1, corresponds to 100%.

CONCLUSIONS

This paper derives the relation between a cable's (or umbilical's) axial tension, the cable elements' axial tension, and friction. In particular, it is emphasized how friction influences the maximum allowable tension (MAT).

A common assumption in the literature is to neglect the influence of friction in the axisymmetric case. Hence, from a theoretical point of view, it can be argued that friction should be neglected when calculating MAT, because MAT by definition is calculated for straight (non-bent) cables.

On the other hand, from a practical point of view, one can argue that a real-life cable is rarely perfectly straight (i.e. has exactly zero bending curvature). Therefore, it may be reasonable to include contribution from friction when calculating MAT.

This paper presents four different approaches for how to handle friction when calculating MAT. These approaches range from neglecting friction in Approach 1 to include the maximum possible friction in Approach 2. Approach 3 and Approach 4 are feasible compromises, where friction is included up to a certain cable bending curvature, which corresponds to an "almost straight" cable, while friction above this limit is disregarded. Approach 4 has the advantage that it can be read directly from the cable's capacity curve (i.e. allowed combinations of axial tension and bending curvature).

All four approaches were applied to the deep-water DEH piggyback cable presented in Figure 1. For this cable, the most conservative approach gives 19% lower MAT than the least conservative approach.

REFERENCES

- [1] A. Nysveen, H. Kulbotten, J. K. Lervik, A. H. Børnes, M. Høyser-Hansen, and J. J. Bremnes. Direct Electrical Heating of Subsea Pipelines - Technology Development and Operating Experience. *IEEE Transactions on Industry Applications*, 43:118 – 129, 2007.
- [2] S. Dretvik and A. H. Børnes. Direct Heated Flowlines in the Åsgard Field. In *Proceedings of the Eleventh (2001) International Offshore and Polar Engineering Conference - Stavanger, Norway*, 2001.
- [3] S. Kvande. Direct Electrical Heating Goes Deeper. *E&P Magazine June 2014*, 2014.
- [4] E. Kebabze. *Theoretical Modelling of Unbonded Flexible Pipe Cross-Sections*. PhD thesis, South Bank University, 2000.
- [5] R. H. Knapp. Derivation of a new stiffness matrix for helically armoured cables considering tension and torsion. *International Journal for Numerical Methods in Engineering*, 14:515 – 529, 1979.
- [6] N. Sødahl, G. Skeie, O. Steinkjær, and A. J. Kalleklev. Efficient fatigue analysis of helix elements in umbilicals and flexible risers. In *Proceedings of the ASME 29th International Conference on Ocean, Offshore and Arctic Engineering OMAE 2010*, 2010.
- [7] M. Lutchansky. Axial stress in armor wires of bent submarine cables. *Journal of Engineering Industry*, 91(3):687 – 693, 1969.